

- Technical Paper -

## FLEXURE BEHAVIOR OF SEGMENTAL CONCRETE BEAMS PRESTRESSED WITH EXTERNAL TENDONS

Chunyakom SIVALEEPUNTH<sup>\*1</sup>, Junichiro NIWA<sup>\*2</sup>, Satoshi TAMURA<sup>\*3</sup> and Yuzuru HAMADA<sup>\*4</sup>

### ABSTRACT

This paper describes the results of an experimental study and nonlinear finite element method in order to examine the flexural behavior and external tendon stress of segmental prestressed concrete beams by varying the length of segment. It is observed that after the opening of segmental joint, the stiffness of such beams considerably decreases. The experimental results are also compared with the externally prestressed monolithic concrete beam and prediction equations for ultimate moment capacity. It is found that the results from the existing prediction equations agree well with the experimental results.

**Keywords:** prestressed concrete, external tendon, precast segment, flexure behavior, segmental length

### 1. INTRODUCTION

Prefabricated segmental concrete bridges with external prestressing, in which the prestressing tendons are placed outside the concrete section and transfer the load to the concrete through end anchorages and deviators, are associated with a span-by-span construction technique that is thought to be the fastest and simplest among this type of construction process. For the construction of each of the spans, the segments are placed one next to the other with epoxy joint, suspended from a beam, and are post-tensioned with external tendons.

With the widely use of external tendons in prestressed concrete structures, an examination of the design and analysis of such structures is needed. The analysis of externally prestressed concrete beams is complicated comparing to the analysis of conventional prestressed concrete beams (i.e. beams prestressed with bonded tendons), because the stress increases in the external tendons, which is depending on the entire deformation of the member and variations of eccentricity of external tendons under the additional load. It is commonly referred as the second-order effects. The stress increment in the external tendon cannot be determined from the conventional strain compatibility as in the case of

bonded tendons, but it must be determined from the analysis of deformation of the entire structure. Several researchers have proposed the equations based on empirical formulations for predicting stresses in unbonded tendons of externally prestressed monolithic concrete beams at ultimate [1], [2]. However, due to the discretization of segmental concrete beams, those equations may need some modification.

The aims of this study were to investigate the flexural behavior by varying the segmental length of segmental concrete beams prestressed with external tendons, to compare the flexure behavior of the segmental concrete beams with the externally prestressed monolithic concrete beams [2], and to check the accuracy of the prediction equations for determining the flexural strength of segmental prestressed concrete beams. This paper addressed the suitable analytical model in nonlinear finite element method (FEM) for evaluating the flexural capacity and tendon stress of segmental prestressed concrete beams in order to confirm its real behavior for further parametric study, such as the location of segmental joint and the number of segments in such beams. The study also compared the experimental results with the prediction equations recommended by AASHTO LRFD design codes [1] and Sivaleepunth, C., et al. [2].

---

\*1 Ph.D. Candidate, Graduate School of Civil Engineering, Tokyo Institute of Technology, JCI Member

\*2 Prof., Dept. of Civil Engineering, Tokyo Institute of Technology, Dr. E., JCI Member

\*3 Research Engineer, Research and Development Center, DPS Bridge Works Co., Ltd., JCI Member

\*4 Manager, Research and Development Center, DPS Bridge Works Co., Ltd., Dr. E., JCI Member

## 2. EXPERIMENTAL PROCEDURES

The test specimens consisted of two concrete beams prestressed with external tendons, with the same total length 3.3 m, cross section dimensions and reinforcement details as shown in Fig. 1a. The specimens were named as F40 and F80 as tabulated in Table 1. For the later specimen, T3\_L10\_S15, the experimental results were obtained from Sivaleepunth, C., et al. [2]. In order to investigate the influence of segmental length, the segmental length was set as 400 mm and 800 mm for specimens F40 and F80,

respectively. The specimen T3\_L10\_S15, adopted for comparison with the experimental results, was cast monolithically. The effective prestress in tendons was around 900 N/mm<sup>2</sup>.

### 2.1 Materials

#### (1) Reinforcements and external tendons

In all specimens, the internal longitudinal tensile reinforcement consisted of two deformed steel bars with nominal diameter of 16 mm ( $A_s = 397.2 \text{ mm}^2$ ), which provided the reinforcement ratio ( $\rho_w = A_s/bd$ ) as 1.13 %, including the area of external tendons, and four deformed steel bars

Table 1 Detail of test beams

Beams	Beam condition	Segmental length (mm)	Effective prestress, $f_{pe}$ (N/mm <sup>2</sup> )	Compressive strength of concrete, $f_c'$ ; batch A (N/mm <sup>2</sup> )	Compressive strength of concrete, $f_c'$ ; batch B (N/mm <sup>2</sup> )	Tensile strength of concrete, $f_t$ ; batch A (N/mm <sup>2</sup> )	Tensile strength of concrete, $f_t$ ; batch B (N/mm <sup>2</sup> )
F40	Segment with epoxy joint	400	934.4	55.8	57.2	4.3	4.8
F80		800	872.8	57.5	56.7	4.4	4.3
T3_L10_S15	Monolithic	-	913.5	56.4		3.6	

Table 2 Mix proportion of concrete

W/C (%)	S/a (%)	Unit weight (kg/m <sup>3</sup> )				SP <sup>*5</sup> (C×%)	AE <sup>*6</sup> (C×%)
		W <sup>*1</sup>	C <sup>*2</sup>	S <sup>*3</sup>	G <sup>*4</sup>		
35.5	38.5	143	403	692	1114	0.65	0.30

\*1 Water

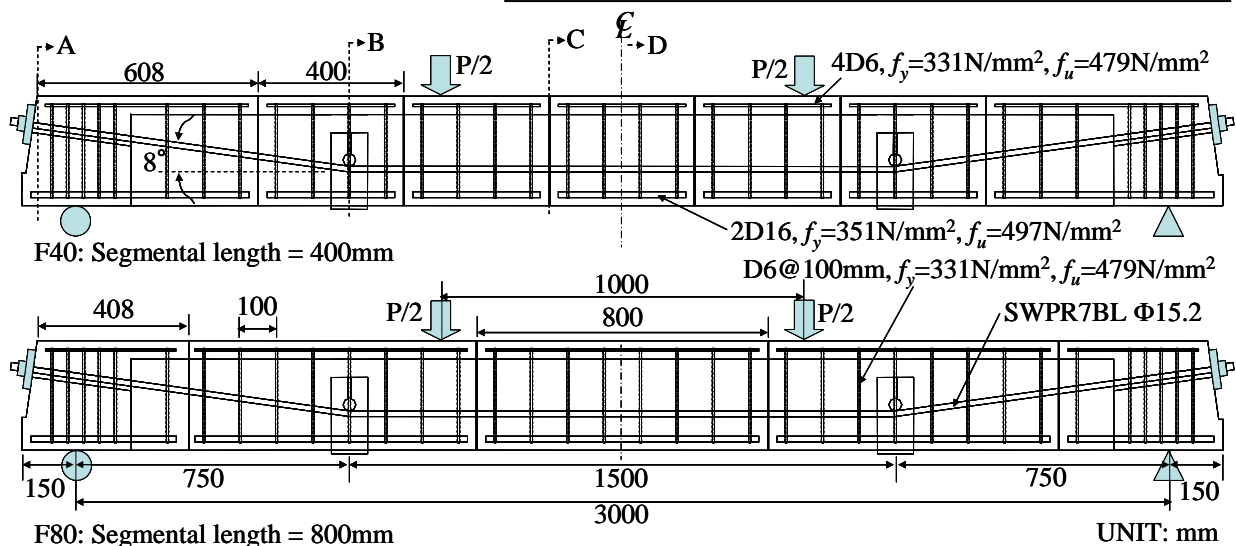
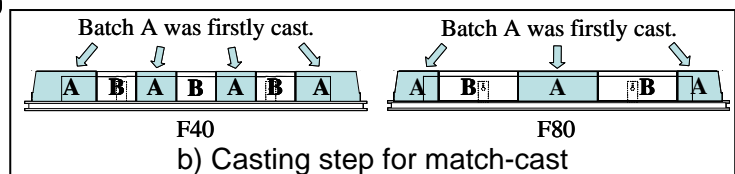
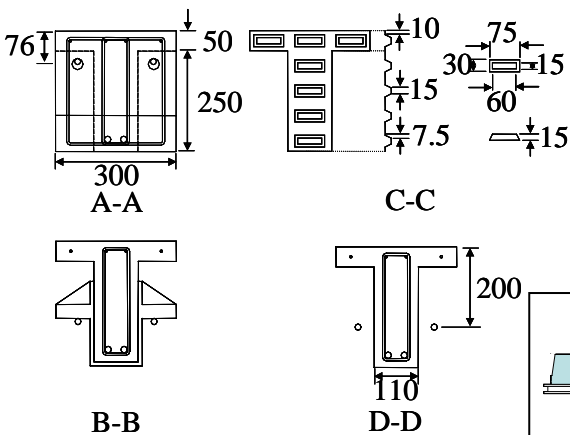
\*2 Ordinary Portland Cement, specific gravity=3.16

\*3 Fine aggregate, specific gravity=2.60, F.M.=2.67

\*4 Coarse aggregate, specific gravity=2.64, F.M.=6.67,  $G_{max}$ =20mm

\*5 Superplasticizer, specific gravity=1.05

\*6 Air-entraining agent, specific gravity=1.02, 100 times dilute solution



a) Dimensions and steel layout of beam specimens  
Fig. 1 Details of specimens

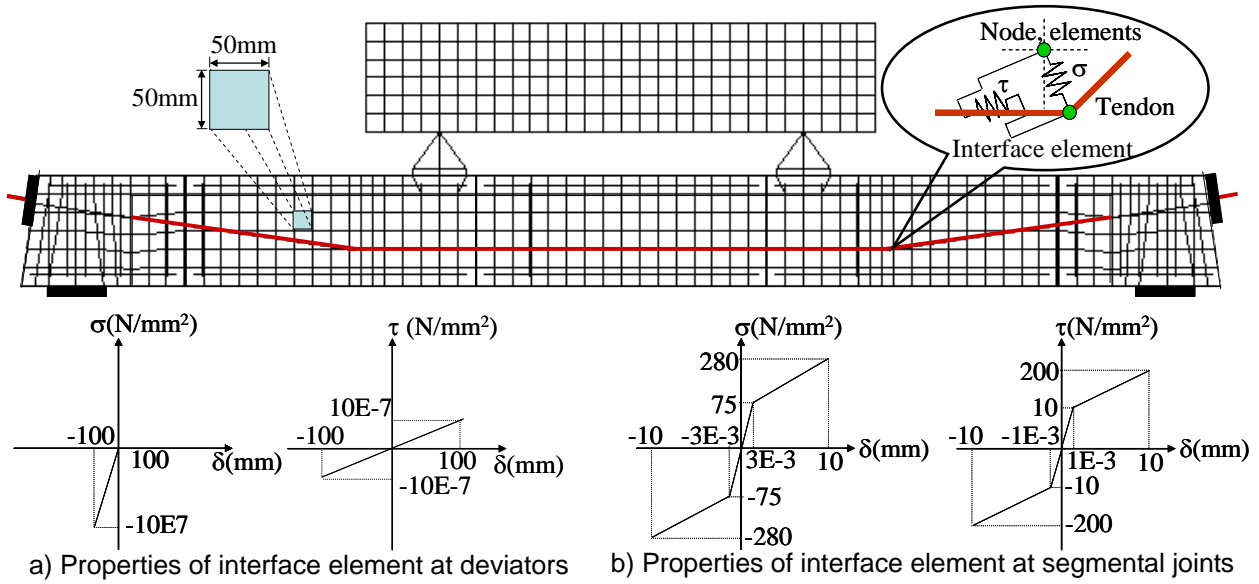


Fig. 2 Finite element analytical model and properties of interface elements

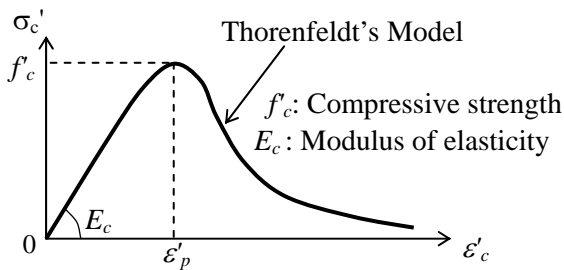


Fig. 3 Compressive model of concrete

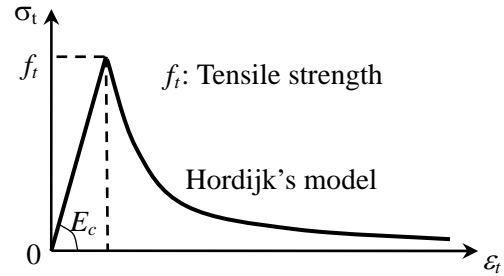


Fig. 4 Tension softening model

were for longitudinal compressive reinforcement with nominal diameter of 6 mm ( $A_s' = 126.7 \text{ mm}^2$ ). Their average yield strength,  $f_y$ , was 351 N/mm<sup>2</sup> and 331 N/mm<sup>2</sup>, average tensile strength,  $f_u$ , was 497 N/mm<sup>2</sup> and 479 N/mm<sup>2</sup>, and modulus of elasticity,  $E_s$ , was 201 kN/mm<sup>2</sup> and 200 kN/mm<sup>2</sup>, respectively. Transverse reinforcement with a nominal diameter of 6 mm ( $A_v = 63.34 \text{ mm}^2$ ) and with yield strength,  $f_{yv}$ , of 331 N/mm<sup>2</sup>,  $E_s$  of 200 kN/mm<sup>2</sup> was provided in a web throughout the length of beams with the spacing,  $s$ , of 100 mm. For external tendons, two straight 7-wire prestressing tendons with a nominal diameter of 15.2 mm ( $A_{ps} = 140.7 \text{ mm}^2$ ) were prepared for each specimen as external tendons. The yield strength,  $f_{py}$ , the tensile strength,  $f_{pu}$ , and the modulus of elasticity of external tendons,  $E_{ps}$ , were 1692 N/mm<sup>2</sup>, 1947 N/mm<sup>2</sup> and 191.2 kN/mm<sup>2</sup>, respectively.

## (2) Concrete and epoxy

Since the segmental concrete beams were adopted in this study, the match-cast technique was utilized; therefore, the concrete was cast for two times in each segmental beam as shown in Fig. 1b. Firstly, the batch A, as shown in Fig. 1b, was cast. After 12 hours of steam curing, the formwork was removed and prepared for batch B.

All batches of the concrete had the same mix proportion as summarized in Table 2. The actual strength of concrete in each batch was measured on the day of testing as tabulated in Table 1. The compressive and tensile strengths of epoxy, which was used at segmental joints, were more than 60 N/mm<sup>2</sup> and 12.5 N/mm<sup>2</sup>, respectively.

## 2.2 Experimental Setup

Before testing, the beam specimens were prestressed using symmetrically arranged external tendons on both sides of the section deviated at 750 mm from the supports by two deviators and anchored at the ends of beams. Teflon sheets were inserted between a specimen and supports and between tendons and deviators for reducing the friction. The electrical strain gauges were placed on three of seven wires of tendons at the midspan of the beam. The strain of the prestressing tendon was taken as its average value. All beams had draped tendon profiles, with a depth of 200 mm at the midspan section. The tendons were stressed to about  $0.45f_{pu}$  as illustrated as the effective prestress,  $f_{pe}$ , in Table 1. The beams were simply supported over a span of 3.0 m and two points loading with a distance between loading points of 1000 mm was provided.

### 3. FEM ANALYSIS

The nonlinear FEM using DIANA system had been conducted in full size of the specimen to examine the flexural behavior of segmental concrete beams prestressed with external tendons. Four node quadrilateral isoparametric plane stress elements in a two dimensional configuration were used for concrete as illustrated in Fig. 2. Since the full size of the specimen is modeled, the loading beam, as shown in Fig. 2, is also modeled with high stiffness to be sure that this loading beam does not fail before the test beam fails. The interface element used at deviators and between each segment is also demonstrated in the figure. The friction between the tendons and the deviators is neglected as shown as  $\tau$  value in Fig. 2(a). As shown in Fig. 2(b), since it is difficult to model the interface element at segmental joints due to the complexity of shear key and epoxy, the interface element between each segment was obtained by varying the stiffness of the model until the load-deflection response can be captured with the experimental results. Two node truss elements are applied as the tendon elements. The reinforcement elements were modeled to have the perfect bond with concrete.

In the analysis, the smeared crack model was adopted as the crack model to concrete elements. For the constitutive model, Thorenfeldt's model [3] was applied for

compression as shown in Fig. 3. After cracking, the tension softening model proposed by Hordijk [4] was utilized as the concrete constitutive model under tension as illustrated in Fig. 4. The yield conditions of Rankine were applied as the tension failure criteria. For the longitudinal reinforcement and prestressing tendons, the bilinear elasto-plastic model of steel was adopted.

### 4. RESULTS AND DISCUSSION

#### 4.1 Crack Patterns and Strain Distribution

The crack patterns of all specimens were demonstrated in Fig. 5. For specimen F80, having longer segmental length, flexural cracks were observed between loading points, where the maximum moment region is, but it could not be observed for specimen F40. However, at the same load with the first flexural crack in specimen F80, the opening of segmental joints in the maximum moment region of specimen F40 could be observed due to the cracks occurred just next to the segmental joints as shown in Fig. 5. It should be noted that the tensile strength of epoxy is higher than the tensile strength of concrete. As the load increased, the segmental joints in specimen F80 also opened. After the joint opening, the only two joints at the midspan increase significantly in width and propagate upward near to the top flange of the beams. The loading was continued until the crushing of

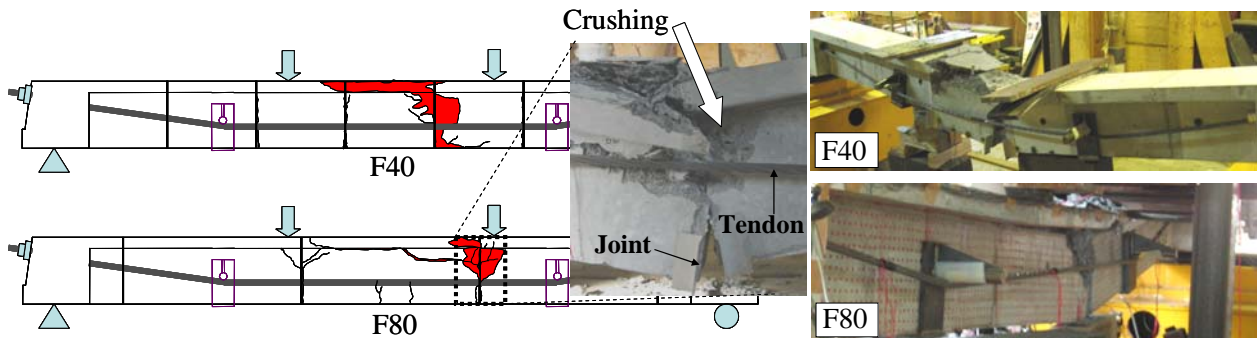


Fig. 5 Crack patterns

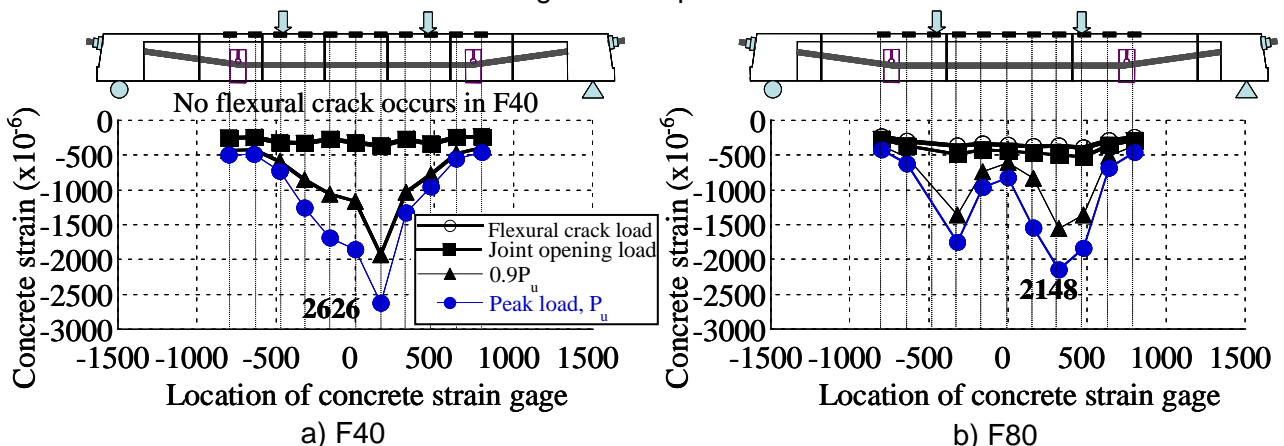


Fig. 6 Distribution of concrete strain

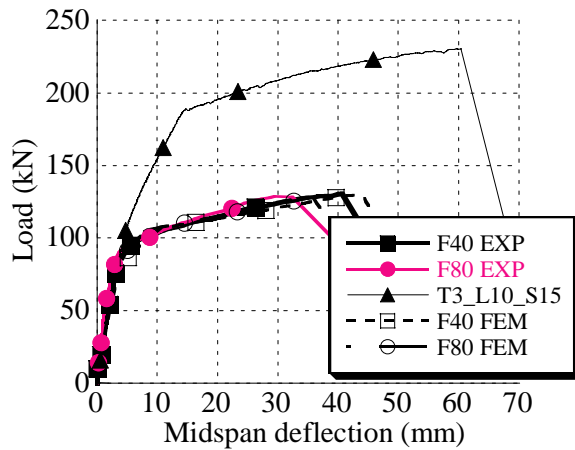


Fig. 7 Load-displacement responses

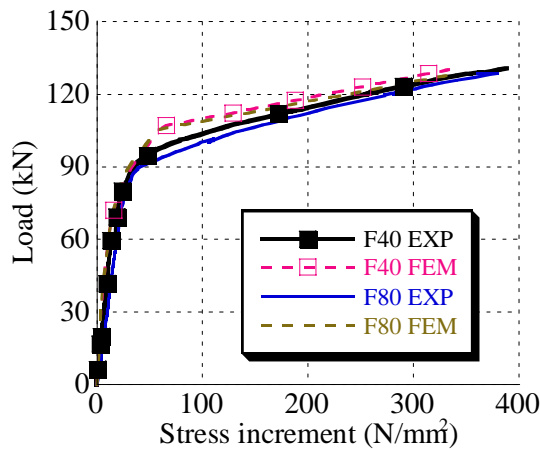


Fig. 8 Load-increase on tendon stress

Table 3 Summary of measured specimens resistance and deformation

Beams	$P_{crack}^{*1}$ (kN)	$P_{joint}^{*2}$ (kN)	$P_u^{*3}$ (kN)	$\delta_u^{*4}$ (mm)	$f_{ps}^{*5}$ (N/mm <sup>2</sup> )	$d_{pu}^{*6}$ (mm)
F40	-	77.1	130.6	40.7	1330.9	184.5
F80	77.1	89.9	128.5	32.5	1251.9	189.5
T3_L10_S15	90	-	230.1	58.3	1451.1	178.9

\*1 Loading resistance at first crack

\*2 Loading resistance at joint opening

\*3 Loading resistance at peak

\*4 Midspan deformation at peak

\*5 Tendon stress at peak

\*6 Tendon level from extreme compressive fiber

concrete near by the segmental joints in the flexural span at the compression zone.

The strain distribution of concrete in the extreme compression fiber at the various loading stage up to failure was presented in Fig. 6. For all specimens, the strain distribution of concrete was fairly uniform until the joint opening load. After the joints opened, only the compressive strain in concrete at or near by segmental joints at the midspan increased considerably. At the peak load, the compressive strain in concrete for all specimens is higher than  $2000 \times 10^{-6}$  near by

segmental joints, which leads to crushing of concrete at that zone.

#### 4.2 Deflection and Stress Increment

The responses of applied load versus deflection and load versus stress increment of beams are illustrated in Figs. 7 and 8, respectively. The summary of measured resistances of specimens from the cracking to the peak load together with the midspan deflection, stress increment in tendon at the peak and tendon depth at the peak are tabulated in Table 3. In the beginning, the beams behaved as the linear elastic body, which made the increase in deflection and stress increment in external tendon very small, until the segmental joints between loading points opened and the stiffness of the beams was reduced. After that the deflection increased with the small increase in load until the ultimate resistance, which makes significant increase of stress increment in external tendons.

#### 4.3 Comparisons with Monolithic Beam and Nonlinear FEM Analytical Results

In this study, the externally prestressed monolithic concrete beam is adopted from Sivaleepunth, C., et al. [2] for the purpose of comparison. All of the specimens had the same dimensions and steel layout. The only difference is that the adopted specimen was monolithically cast, but the specimens in this study were cast in segment. Figures 7 and 8 demonstrate the comparison of those beams for load-deflection curve and load-stress increment in external tendons curve, respectively. It can be observed that the initial stiffness of all beams was the same; however, after the segmental joints opened, the stiffness suddenly dropped for segmental beams. The stiffness of a monolithic beam gradually decreased due to the flexural crack. In a monolithic beam, when the load reached the yield strength of internal bonded tensile reinforcement, the beam stiffness decreased again, and had similar slope as in segmental beams. The peak loads of segmental beams were about 50% of a monolithic beam due to the compressive stress concentration near the segmental joints in the maximum moment region.

The analytical method presented earlier was used to predict the responses of the segmental beams. It is shown in Figs. 7 and 8 that the analytical results provide the well-predicted results compared with the experimental results. This is proven that the analytical model in nonlinear FEM coincides with the response of segmental prestressed concrete beams, which can lead to the extension of other parameters for further study.

## 5. COMPARISON WITH THE PREDICTION EQUATIONS

As expressed in the previous section, the numerical solution techniques can be used to predict the tendon stress. However, a simplified method for predicting the maximum moment resistance is needed for the practical design. This paper shows the accuracy in prediction of the existing prediction equations [1], [2] with the presented experimental results.

The maximum moment resistance,  $M_u$ , can be computed if the stress in external tendons,  $f_{ps}$ , at the peak load is available. Therefore, many researchers proposed prediction equations for evaluating the tendon stress at ultimate.

AASHTO LRFD Bridge Design suggests a stress in unbonded tendons of flexural members in term of bond reduction factor,  $\Omega_u$ . It can be obtained from the following expression:

$$f_{ps} = f_{pe} + \Omega_u E_{ps} \varepsilon_{cu} \left( \frac{d_{ps}}{x} - 1 \right) < 0.94 f_{py} \quad (1)$$

where,  $\Omega_u = \frac{1.5}{(L/d_{ps})}$  for one-point loading; (2)

$$\Omega_u = \frac{3}{(L/d_{ps})} \text{ for third-point loading (3)}$$

Sivaleepunth, C., et al. proposed the prediction equation by modifying the bond reduction factor [2] and adopting the formulation of depth reduction factor,  $R_d$ , from Aravinthan, T. [5]. The loading distance to the span length,  $L_d/L$ , is considered for evaluating the tendon stress.

$$f_{ps} = f_{pe} + \Omega_u E_{ps} \varepsilon_{cu} \left( \frac{d_{pu}}{x} - 1 \right) \leq f_{py} \quad (4)$$

where,  $\Omega_u = 0.3 \left( \frac{L_d}{L} \right) + 0.01 \left( \frac{S_d}{d_{ps}} \right) + 0.1$  (5)

$$d_{pu} = R_d d_{ps} \quad (6)$$

Table 4 illustrates the calculated results of the maximum moment resistance from AASHTO

Table 4 Comparison with prediction equations

Beams	EXP	AASHTO [1]		Sivaleepunth[2]	
	$M_u$ kN-m	$M_u$ kN-m	$M_{u,CAL}/M_{u,EXP}$	$M_u$ kN-m	$M_{u,CAL}/M_{u,EXP}$
F40	65.3	72.0	1.10	67.9	1.04
F80	64.2	70.0	1.09	66.2	1.03
T3_L10_S15	115.1	103.5	0.90	99.4	0.86
Average	-	-	1.03	-	0.98

and Sivaleepunth, C., et al. It can be observed that both formulations can provide reasonable results with the average value of  $M_{u,CAL}/M_{u,EXP}$  as 1.03 and 0.98 for AASHTO and Sivaleepunth, C., et al., respectively. From these results, it is proven that the prediction equations, which were proposed based on the ultimate capacity of monolithic beams, can also be applied to segmental concrete beams prestressed with external tendons by neglecting the discontinuity of internal longitudinal reinforcements (i.e.  $A_s$  and  $A_s' = 0$ ).

## 6. CONCLUSIONS

- (1) The segmental length has less significant effect to the flexural capacity of the beams according to the experimental and analytical results in this study.
- (2) The flexural capacity of segmental beams is lower than that of a monolithic beam due to the discontinuity of internal bonded reinforcement in segmental beams.
- (3) After the segmental joints opened, the compressive stress concentrates near to the top of opened segmental joints, which causes the compression failure at that region.
- (4) The analytical model of nonlinear FEM is applicable to examine the flexural behavior of segmental concrete beams.
- (5) The existing prediction equations for flexural resistance can provide the good agreement with experimental results.

## REFERENCES

- [1] AASHTO LRFD: Bridge Design Specifications SI Units First Edition, 1994
- [2] Sivaleepunth, C., Niwa, J., Bui, K.D., Tamura, S. and Hamada, Y.: Prediction of Tendon Stress and Flexural Strength of Externally Prestressed Concrete Beams, Journal of Materials, Concrete Structures and Pavements, V-62(1), pp. 260-273, 2006
- [3] Thorenfeldt, E., Tomaszewicz, A. and Jensen, J. J.: Mechanical Properties of High-strength Concrete and Applications in Design, Symposium Proceedings of Utilization of High-strength Concrete, Norway, 1987
- [4] Hordijk, D. A.: Local Approach to Fatigue of Concrete, PhD thesis, Delft University of Technology, 1991
- [5] Aravinthan, T.: Flexural Behavior and Design Methodology of Externally Prestressed Concrete Beams, PhD thesis, Saitama University, 1999